Science Translational Medicine
AAAS

www.sciencetranslationalmedicine.org/cgi/content/full/8/370/370ra181/DC1

# Supplementary Materials for

## Adenylyl cyclase activating polypeptide reduces phosphorylation and toxicity of the polyglutamine-expanded androgen receptor in spinobulbar muscular atrophy

Maria Josè Polanco, Sara Parodi, Diana Piol, Conor Stack, Mathilde Chivet, Andrea Contestabile, Helen C. Miranda, Patricia M.-J. Lievens, Stefano Espinoza, Tobias Jochum, Anna Rocchi, Christopher Grunseich, Raul R. Gainetdinov, Andrew C. B. Cato, Andrew P. Lieberman, Albert R. La Spada, Fabio Sambataro, Kenneth H. Fischbeck, Illana Gozes, Maria Pennuto*

*Corresponding author. Email: mpennuto@dti.telethon.it

Published 21 December 2016, *Sci. Transl. Med.* **8**, 370ra181 (2016)
DOI: 10.1126/scitranslmed.aaf9526

**This PDF file includes:**

**Table S1. List of PACAP analogs and cAMP release in MN-1 cells treated with either PACAP or the indicated PACAP analogs.**

Peptide 1: Stearyl-Lys-Lys-Tyr-Leu-$NH_2$

Peptide 2: HSDGIFTDSYSRYRKQ-Nle-AVKKYLAAVL-$NH_2$

Peptide 3: HSDAVFTDNYTRLRKQ-Nle-AVKKYLNSILN-$NH_2$

Peptide 4: HSDGIFTDSYSRYRKQ-Nle-AVKKYLAAVLGKRYKQRVKNK-$NH_2$

Peptide 5: ACETYL- HSDGIFTDSYSRYRKQ-Nle-AVKKYLAAVLGKRYKQRVKNK-$NH_2$

Peptide 6: ACETYL-HSDGIFTDSYSRYRAQMAVAKYLAAVLGKRYKQRVKNK- PROPYLAMID

Peptide 7: ACETYL-HSDGIFTDSYSRYRAQMAVAKYLAAVLGKRYKQRVKNK-OH

**cAMP release in MN-1 cells treated with either PACAP or the indicated PACAP analogs.**

EC50 (nM) of PACAP and the PACAP analogs described in Table 1 measured by BRET assay in MN-1 cells expressing AR24Q and AR65Q and treated with either vehicle or DHT (10 nM) for 24 h.

| | AR24Q | AR24Q | AR65Q | AR65Q |
|---|---|---|---|---|
| | Vehicle | DHT | Vehicle | DHT |
| PACAP | 0.24 | 0.23 | 0.18 | 0.27 |
| PEPTIDE 1 | 630 | 470 | 250 | 387 |
| PEPTIDE 2 | 0.38 | 0.59 | 0.17 | 0.26 |
| PEPTIDE 3 | 250 | 290 | 110 | 220 |
| PEPTIDE 4 | 0.49 | 0.48 | 0.32 | 0.32 |
| PEPTIDE 5 | 0.76 | 0.60 | 0.71 | 0.57 |
| PEPTIDE 6 | 2.4 | 2.4 | 4 | 3.2 |
| PEPTIDE 7 | 0.22 | 0.34 | 0.38 | 0.31 |

**Fig. S1**

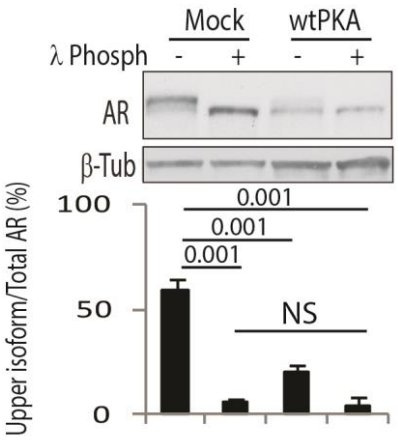


**Fig. S1. Overexpression of PKA reduces the accumulation of the upper isoform of polyQ-AR.** Western blotting analysis of AR55Q in HEK293T cells transfected with empty vector (Mock) and vector expressing wtPKA. Cell extracts were incubated with λ phosphatase (λ phosph). AR was detected with a specific antibody, and beta-tubulin (β-Tub) was used as loading control. Graph, mean ± SEM, *N* = 3 independent experiments. One-way ANOVA. NS, non-significant.

**Fig. S2**

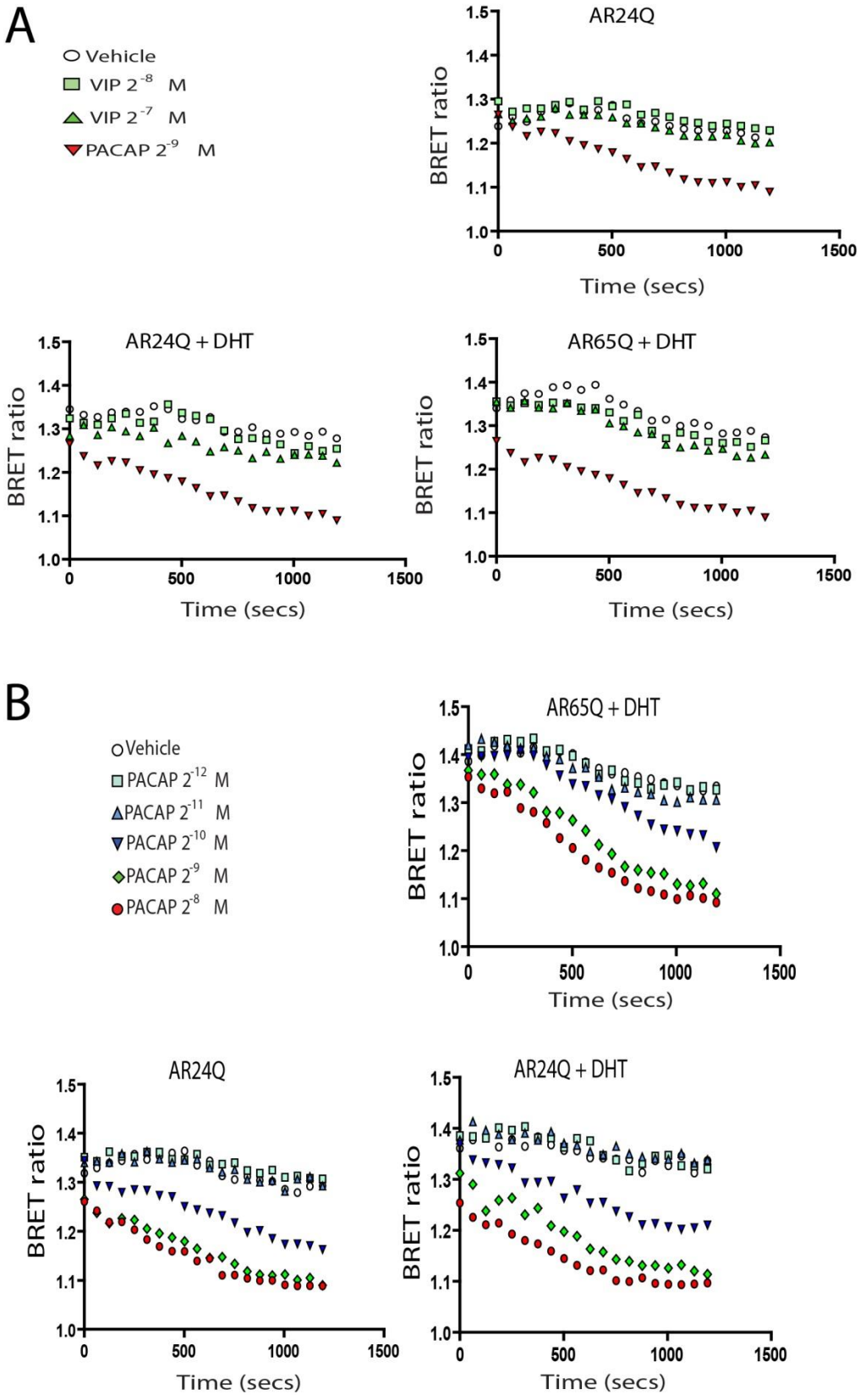


**Fig. S2. PACAP stimulates the release of cAMP in MN-1 cells expressing AR24Q and AR65Q.** A-B) BRET analysis of cAMP release in the MN-1 cells treated as indicated. PACAP induced cAMP release and its effect was dose-dependent. *N* = 3 independent experiments.

**Fig. S3**

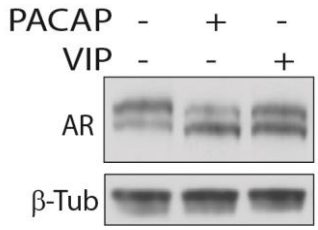


**Fig. S3. VIP does not modify the accumulation of the upper isoform of polyQ-AR.**
Western blotting analysis of AR55Q in HEK293T cells treated with PACAP (100 nM) and VIP (100 nM) for 5 h. PACAP, and not VIP, reduced the accumulation of the upper isoform of polyQ-AR. AR was detected with a specific antibody, and beta- tubulin (β-Tub) was used as loading control. *N* = 3 independent experiments.

**Fig. S4**

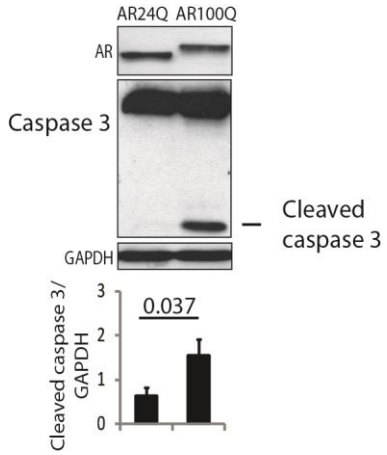


**Fig. S4. Expression of polyQ-AR in MN-1 cells results in caspase 3 activation.**
Western blotting analysis of caspase 3 proteolytic cleavage in MN-1 cells stably expressing either AR24Q or AR100Q treated with DHT (10 nM) for 72 h. AR and caspase 3 were detected with specific antibodies, and GAPDH was used as loading control. Graph, mean ± SEM, *N* = 7 independent experiments. Student's t test.

**Fig. S5**

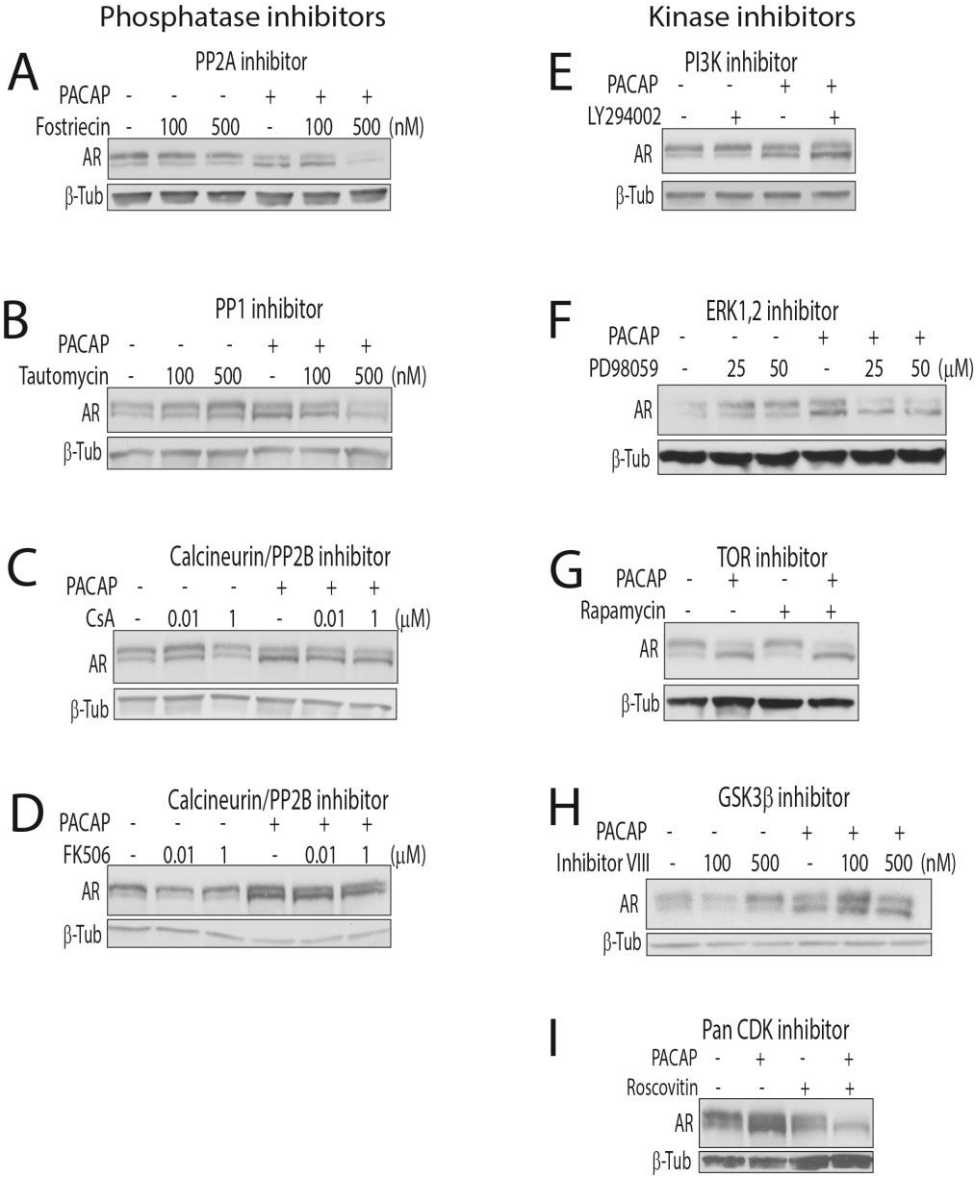


**Fig. S5. Analysis of polyQ-AR phosphorylation upon inhibition of specific cellular phosphatases and kinases.**

A-D) Western blotting analysis of AR55Q in HEK293T cells treated with PACAP (100 nM) and specific phosphatase inhibitors: fostriecin (PP2A inhibitor), tautomycin (PP1 inhibitor), and cyclosporine A (CsA) and FK506 (PP2B inhibitors) for 5h. Inhibition of these phosphatases did not alter the accumulation of the upper isoform of polyQ-AR, nor did it block the effect of PACAP.

E-I) Western blotting analysis of AR55Q in HEK293T cells treated with PACAP (100 nM) and specific kinase inhibitors: LY294002 (40 μM) (PI3K inhibitor), PD98059 (50 μM) (ERK1/2 inhibitor), rapamycin (100 nM) (mTOR inhibitor), inhibitor VIII (GSK3β inhibitor), and roscovitin (20 μM) (pan-CDK inhibitor) for 5 h. Inhibition of PI3K, ERK1/2, mTOR, and GSK3β did not modify the accumulation of the upper isoform of polyQ-AR, and it did not block the PACAP effect on polyQ-AR phosphorylation. On the other hand, roscovitin decreased the accumulation of the upper isoform of polyQ-AR, indicating that a CDK is involved in the regulation of polyQ-AR phosphorylation.

AR was detected with a specific antibody, and beta-tubulin (β-Tub) was used as loading control. *N* = 3 independent experiments.

**Fig. S6**

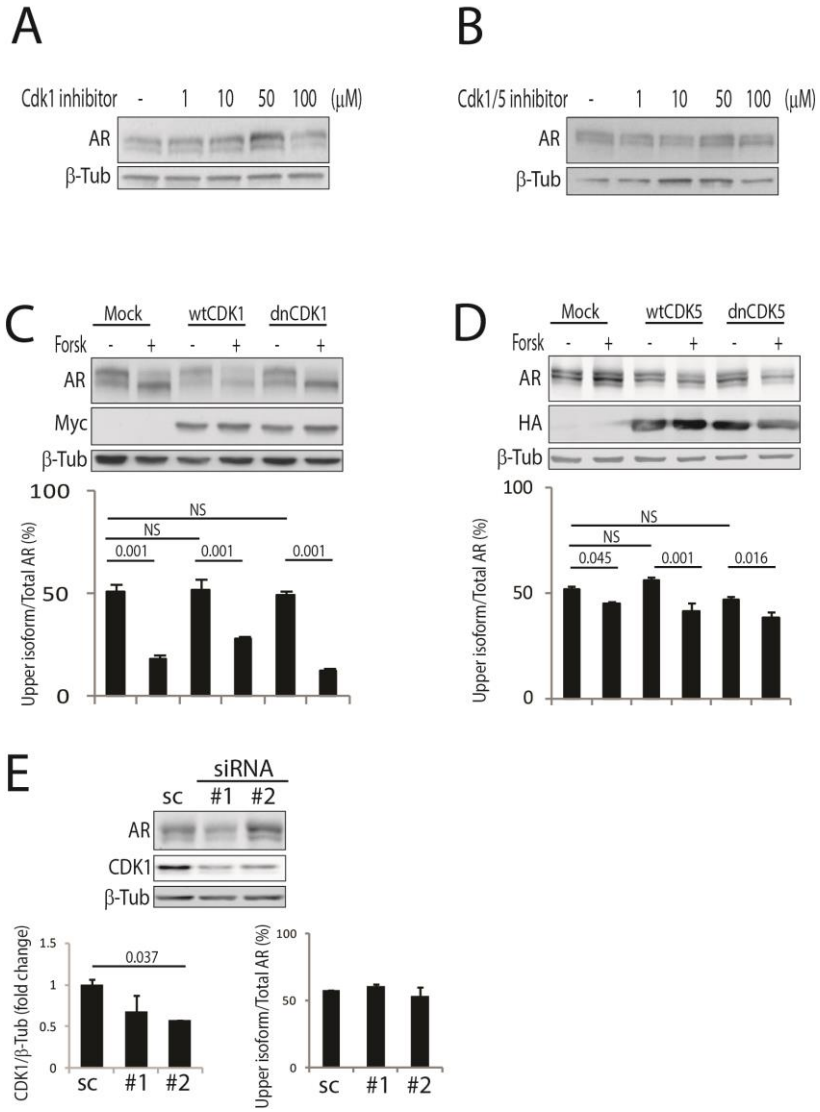


**Fig. S6. Modulation of CDK1 and CDK5 activity does not affect the accumulation of the upper isoform of polyQ-AR.**

A-B) Western blotting analysis of AR55Q in HEK293T cells treated with inhibitors targeting CDK1 and CDK5 for 5 h. Inhibition of either CDK1 or CDK5 did not modify the accumulation of the upper isoform of polyQ-AR. *N* = 3 independent experiments.

C) Western blotting analysis in HEK293T cells transfected with vector expressing AR55Q together with empty vector (Mock), and vectors expressing Myc-tagged wtCDK1 and dnCDK1. The cells were treated with either vehicle or forskolin (Forsk, 10 μM) for 5 h. Graph, mean ± SEM, *N* = 3 independent experiments. NS, non-significant.

D) Western blotting analysis in HEK293T cells transfected with vector expressing AR55Q together with empty vector (Mock), and vectors expressing HA-tagged wtCDK5 and dnCDK5 and treated with forskolin (Forsk, 10 μM) for 5 h. Graph, mean ± SEM, *N* = 3 independent experiments. NS, non-significant.

**E**) Western blotting analysis in HEK293T cells expressing AR55Q together with either scrambled (sc) siRNA or two different siRNAs against endogenous CDK1. Graph, mean ± SD, *N* = 2 independent experiments.

AR, Myc-tagged CDK1, and HA-tagged CDK5 were detected with specific antibodies, and beta-tubulin (β-Tub) was used as loading control. One-way ANOVA.

**Fig. S7**

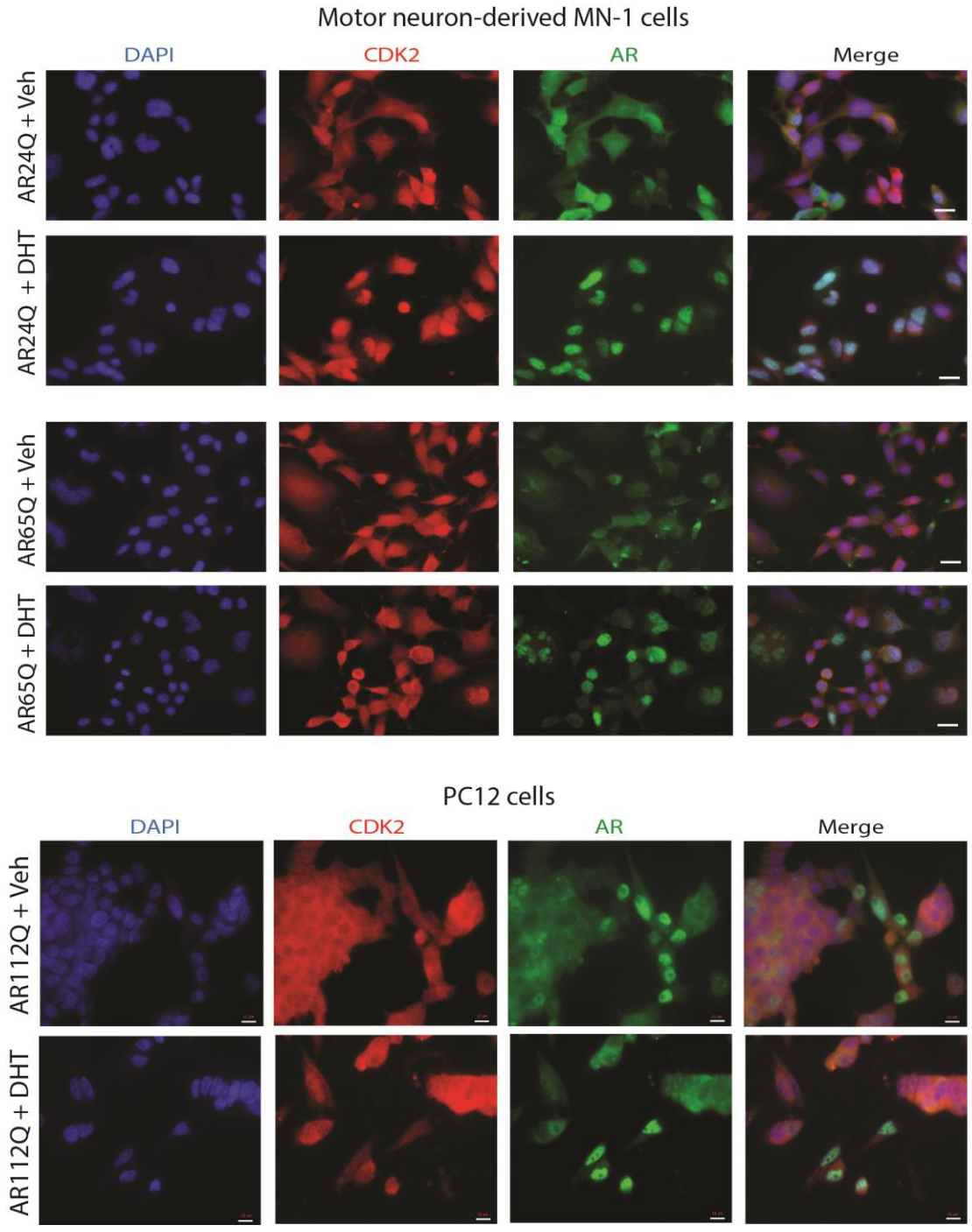


**Fig. S7. Nonexpanded AR and polyQ-AR colocalize with endogenous CDK2 in the absence and presence of androgens in MN-1 and PC12 cells.**

Immunofluorescence analysis of AR (green), CDK2 (red), and nuclei (blue) in motor neuron-derived MN-1 cells stably expressing AR24Q and AR65Q, and doxycycline-inducible PC12 cells stably expressing AR112Q. The MN-1 cells were treated with vehicle (Veh) and DHT (10 nM) for 24 h. The PC12 cells were treated with doxycycline (10 μg/ml), vehicle (Veh) and DHT (50 μM) for 72 h. AR and CDK2 were detected with specific antibodies, and nuclei were stained with DAPI. *N* = 3 independent experiments. Scale bar, MN-1: 20 μm; PC12: 10 μm.

**Fig. S8**

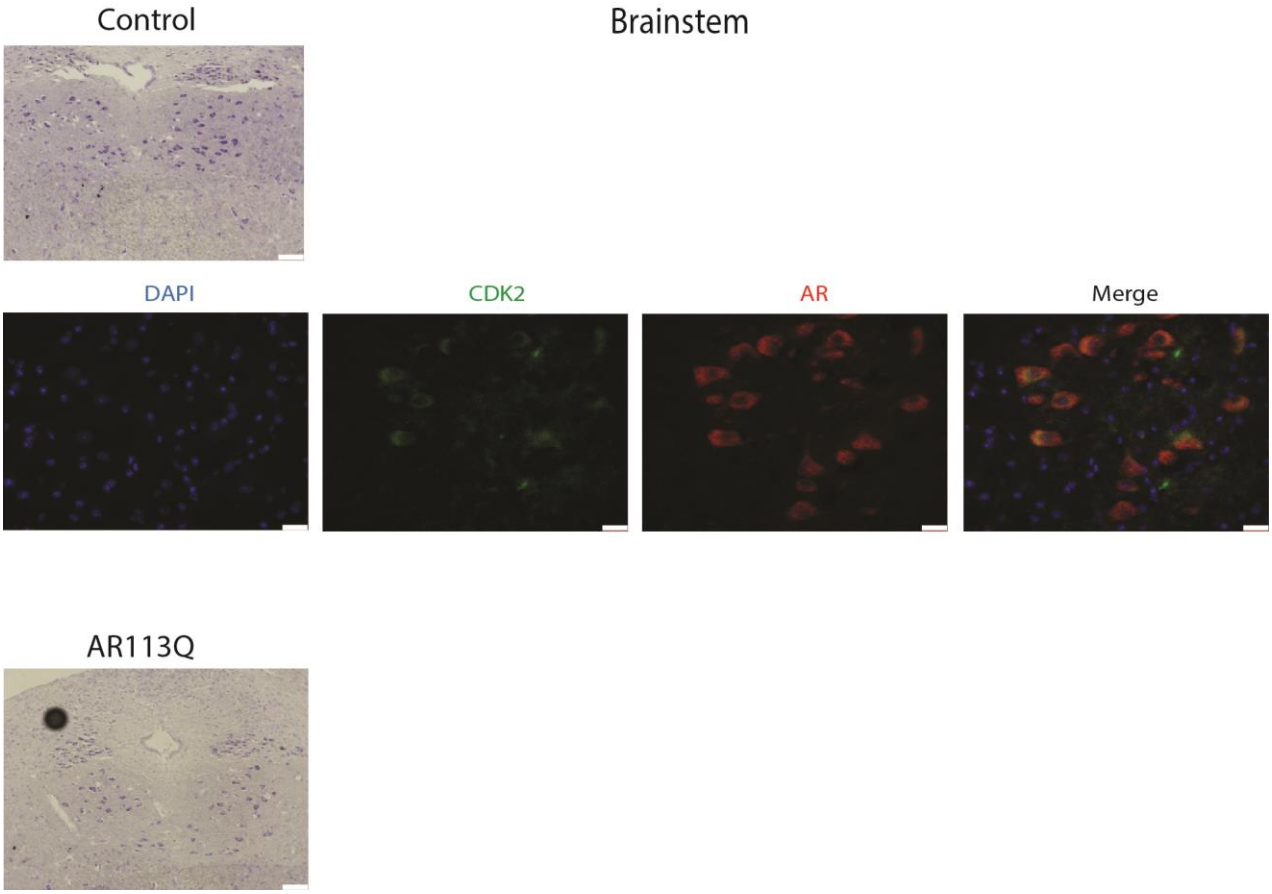


**Fig. S8. Nonexpanded AR and polyQ-AR colocalize with endogenous CDK2 in the brainstem motor neurons of control and knock-in SBMA mice.**
Top panels: Nissl staining. Bottom panels: Immunofluorescence analysis of AR (red), CDK2 (green), and nuclei (DAPI, blue) in the brainstem of 180-day-old control (wild type) and AR113Q mice. Immunofluorescence analysis of AR113Q is shown in the main text. *N* = 3 independent experiments. Scale bar, 25 μm.

**Fig. S9**

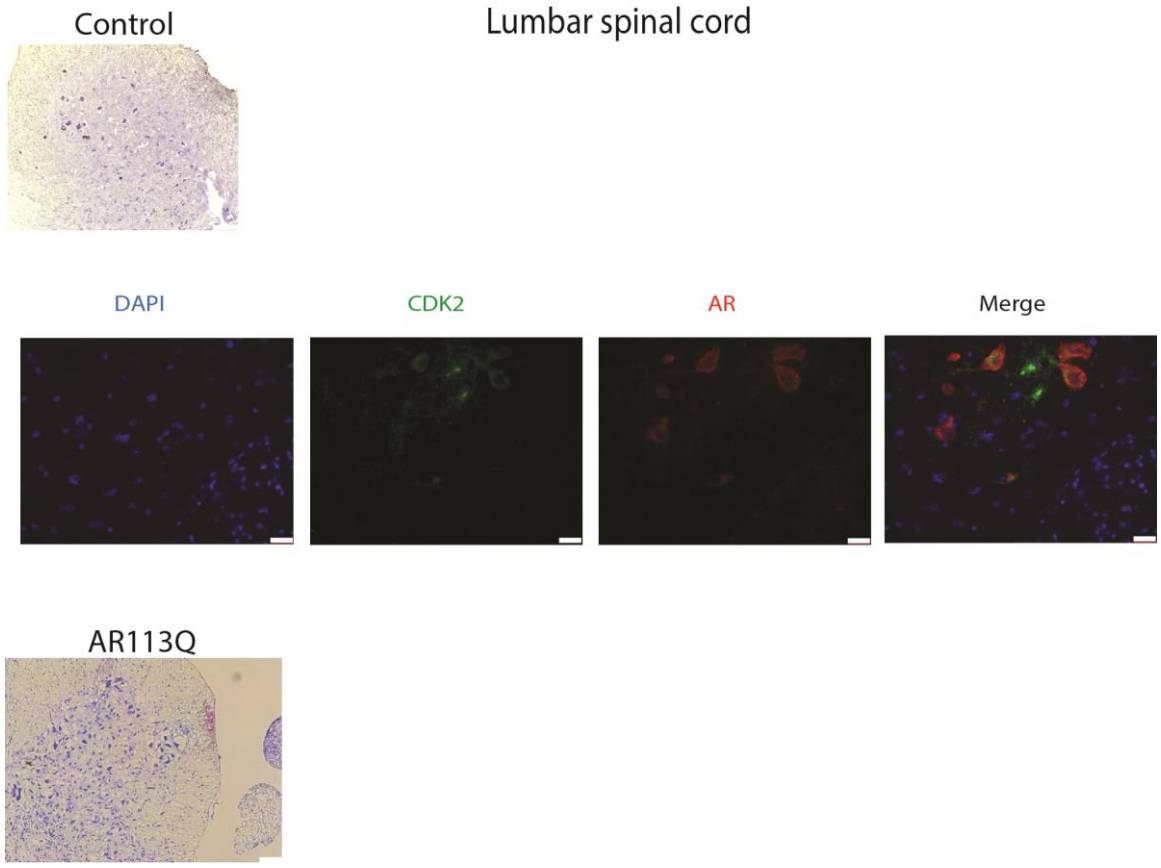


**Fig. S9. Nonexpanded AR and polyQ-AR colocalize with endogenous CDK2 in the motor neurons of the lumbar spinal cord of control and knock-in SBMA mice.**
Top panels: Nissl staining. Bottom panels: Immunofluorescence analysis of AR (red), CDK2 (green), and nuclei (DAPI, blue) in the lumbar spinal cord of 180-day-old control and AR113Q mice. Immunofluorescence analysis of AR113Q is shown in the main text. *N* = 3 independent experiments. Scale bar, 25 μm.

**Fig. S10**

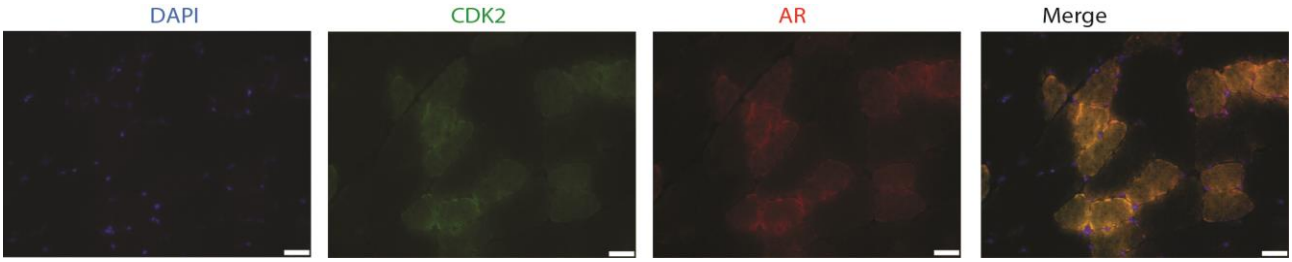


**Fig. S10. Nonexpanded AR colocalizes with endogenous CDK2 in the quadriceps of control mice.**

Immunofluorescence analysis of AR (red), CDK2 (green), and nuclei (DAPI, blue) in the quadriceps muscle of 180-day-old control (wild type) mice. *N* = 3 independent experiments. Scale bar, 100 μm.

**Fig. S11**

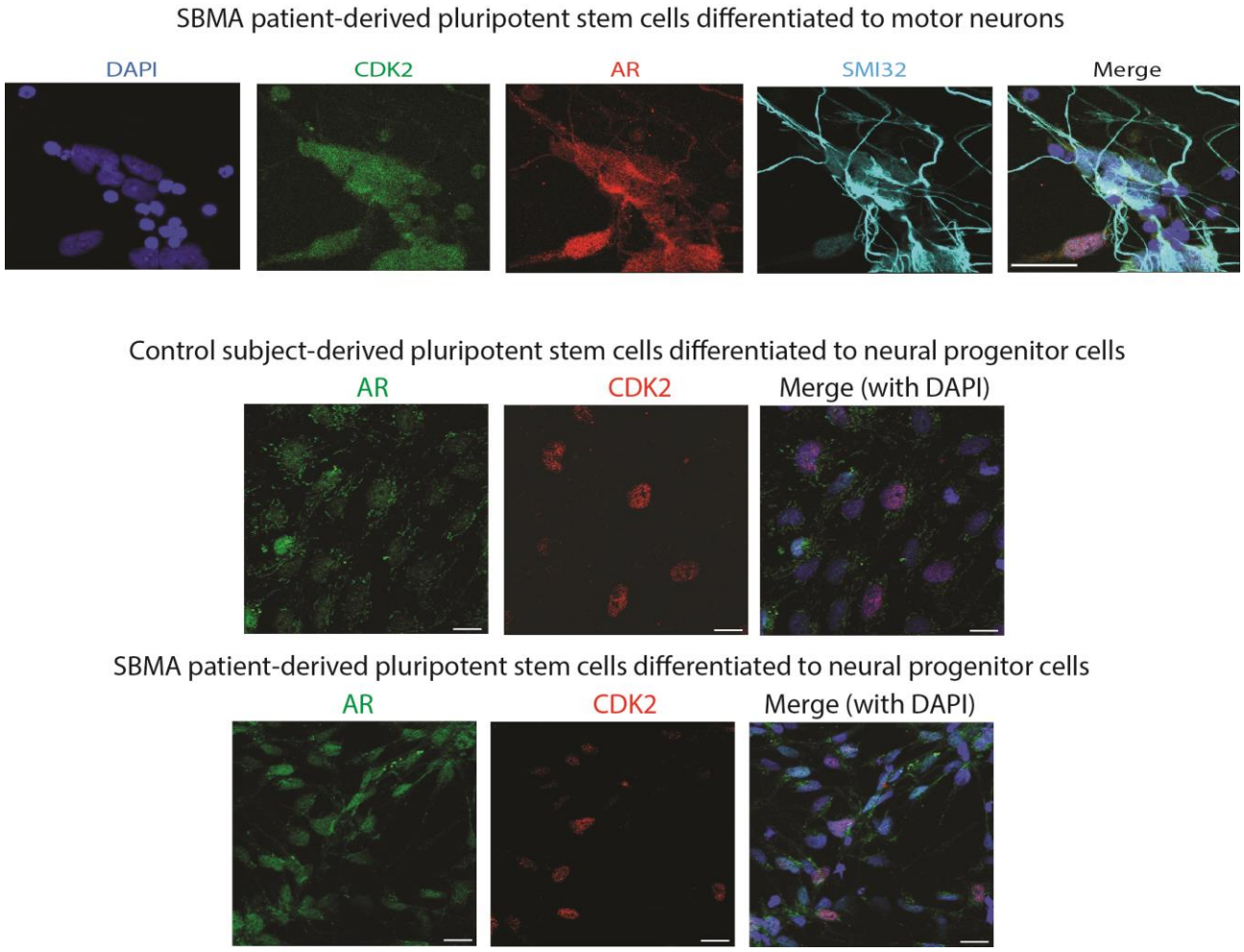


**Fig. S11. Endogenous nonexpanded AR and polyQ-AR colocalize with endogenous CDK2 in control and SBMA patient-derived motor neurons and NPCs.**
Immunofluorescence analysis of endogenous AR and CDK2 in SBMA patient-derived IPSCs differentiated to motor neurons for 7 DIV (days *in vitro*) in the presence of DHT (10 nM), and in control subject- and SBMA patient-derived neural progenitor cells (NPCs). AR (green), CDK2 (red), and the motor neuron marker SMI32 (cyan) were detected with specific antibodies, and nuclei (blue) were stained with DAPI. $N = 3$ independent experiments. Scale bar, motor neurons: 25 μm; NPCs: 10 μm.

**Fig. S12**

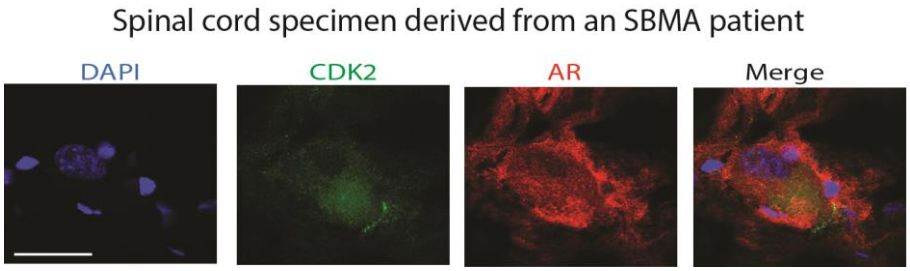


**Fig. S12. Endogenous polyQ-AR colocalizes with endogenous CDK2 in the spinal cord of an SBMA patient.**

Immunofluorescence analysis of endogenous polyQ-AR and CDK2 in the spinal cord of an SBMA patient. Nuclei were stained with DAPI; CDK2 (green) and AR (red) were detected with specific antibodies. Bar, 25 microns.

**Fig. S13**

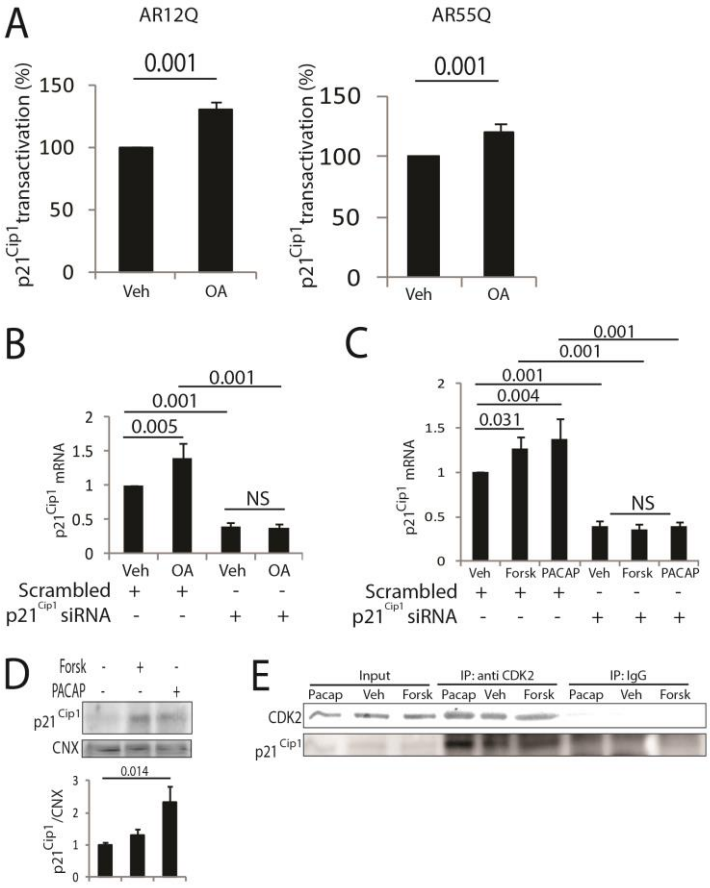


**Fig. S13. Forskolin, PACAP, and the pan-phosphatase inhibitor OA stimulate p21$^{Cip1}$ expression.**

A) Luciferase assay in HEK293T cells transfected with vectors expressing either non-expanded AR (AR12Q) or polyQ-AR (AR55Q) and the luciferase reporter gene under the control of the p21$^{Cip1}$ promoter. The cells were treated with vehicle (veh) and okadaic acid (OA, 5 nM) for 24 h. Treatment of the cells with OA resulted in activation of the p21$^{Cip1}$ promoter. *N* = 4 independent experiments.

B) Real-time PCR analysis of *p21$^{Cip1}$* transcript levels normalized to actin in HEK293T cells transfected with either scrambled siRNA or siRNA against p21$^{Cip1}$ and treated with vehicle (veh) and OA (5 nM) for 24 h. *N* = 4-6 independent experiments.

C) Real-time PCR analysis of *p21$^{Cip1}$* transcript levels normalized to actin in HEK293T cells transfected with either scrambled siRNA or siRNA against p21$^{Cip1}$ and treated with vehicle (veh), forskolin (Forsk, 10 μM), and PACAP (100 nM) for 24 h. *N* = 4-6 independent experiments.

D) Western blotting analysis of p21$^{Cip1}$ expression in MN-1 cells treated with (Forsk, 10 μM) and PACAP (100 nM) for 7 h. Because p21$^{Cip1}$ has a very short half-life, all samples were treated with MG132 (10 μM) to increase the basal levels of p21$^{Cip1}$. *N* = 4 independent experiments.

E) Immunoprecipitation (IP) analysis in MN-1 cells expressing AR100Q and treated with MG132, PACAP, and forskolin, as indicated, and immunoblotting analysis of endogenous CDK2 and p21$^{Cip1}$. Input, 10% of total protein extract. *N* = 2 independent experiments.

Graph, mean ± SEM, Student's t test (A), one-way ANOVA (B-D). NS, non-significant.

**Fig. S14**

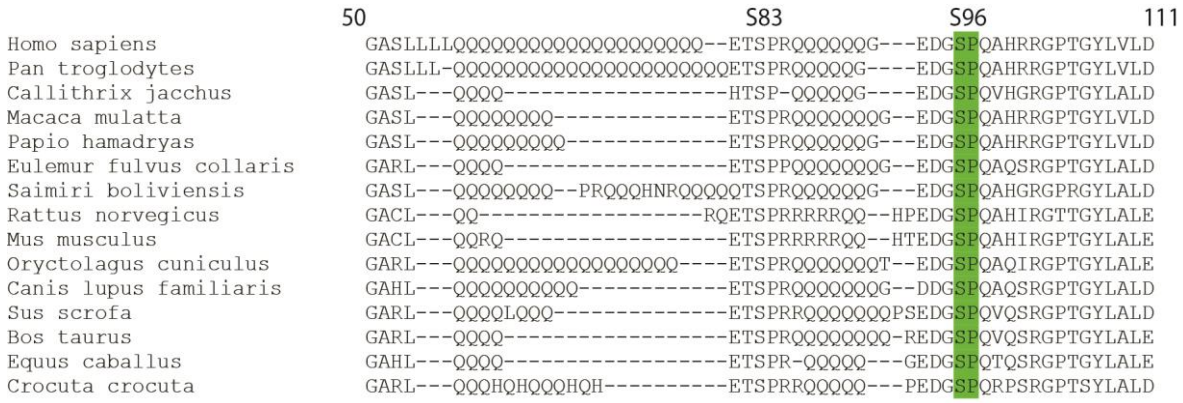


**Fig. S14. Ser$^{96}$ of AR is conserved throughout evolution.**
Alignment of the AR fragment spanning residues 50 to 111 (human AR, NM_000044) shows that serine 96 is conserved throughout evolution.

**Fig. S15**

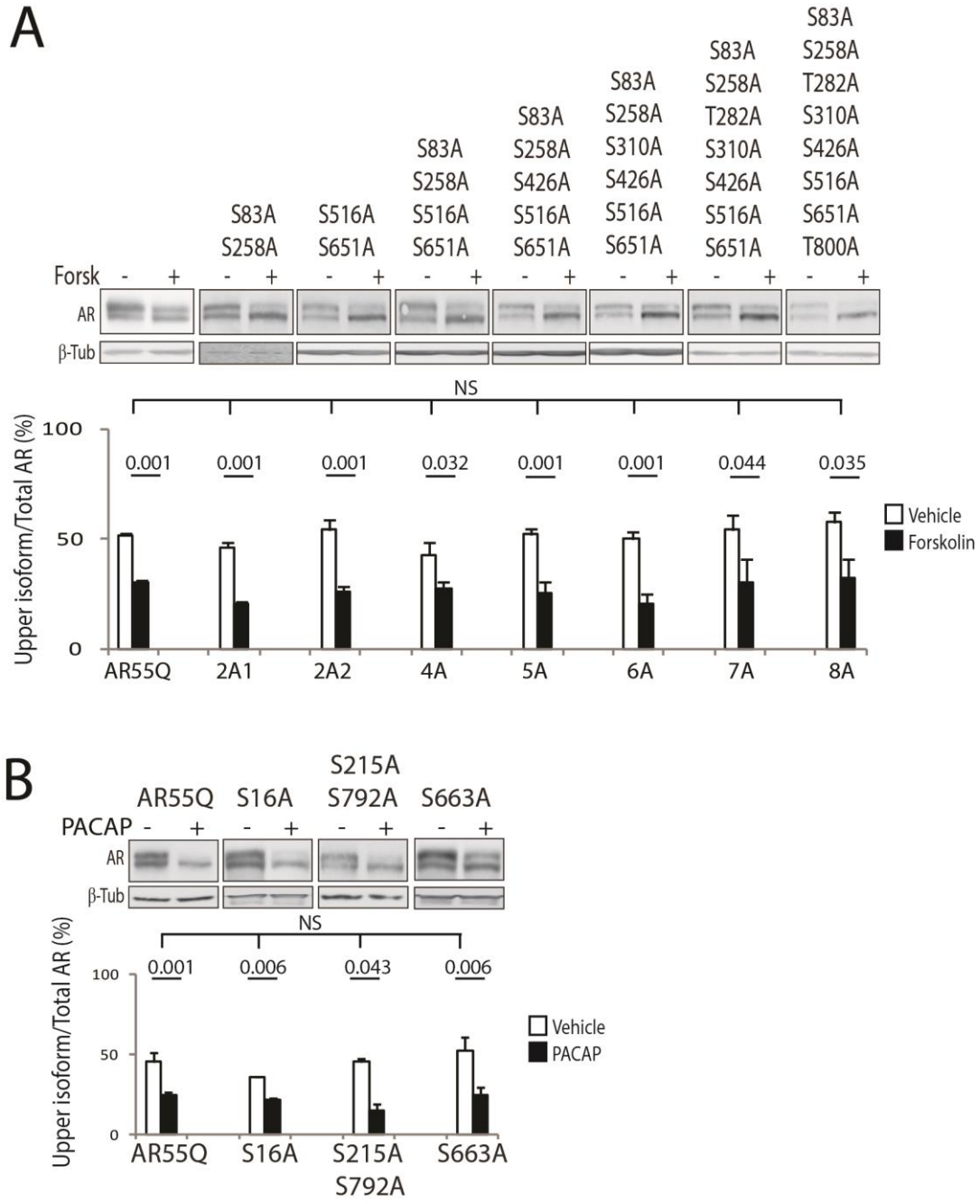


**Fig. S15. Analysis of phosphoresistant polyQ-AR variants.**

A-B) Western blotting analysis of the indicated serine-to-alanine phospho-resistant polyQ-AR variants in HEK293T cells treated with vehicle, forskolin (10 μM), and PACAP (100 nM) for 5 h. Loss of phosphorylation at the indicated residues (NM_000044) neither mimicked S96A nor it altered forskolin and PACAP effect on the accumulation of the upper AR isoform, suggesting that phosphorylation at these sites is not responsible for the formation of the upper isoform of polyQ-AR. AR was detected with a specific antibody, and beta-tubulin (β-Tub) was used as loading control. Graph, mean ± SEM, *N* = 3 independent experiments, One-way ANOVA. NS, non-significant.

**Fig. S16**

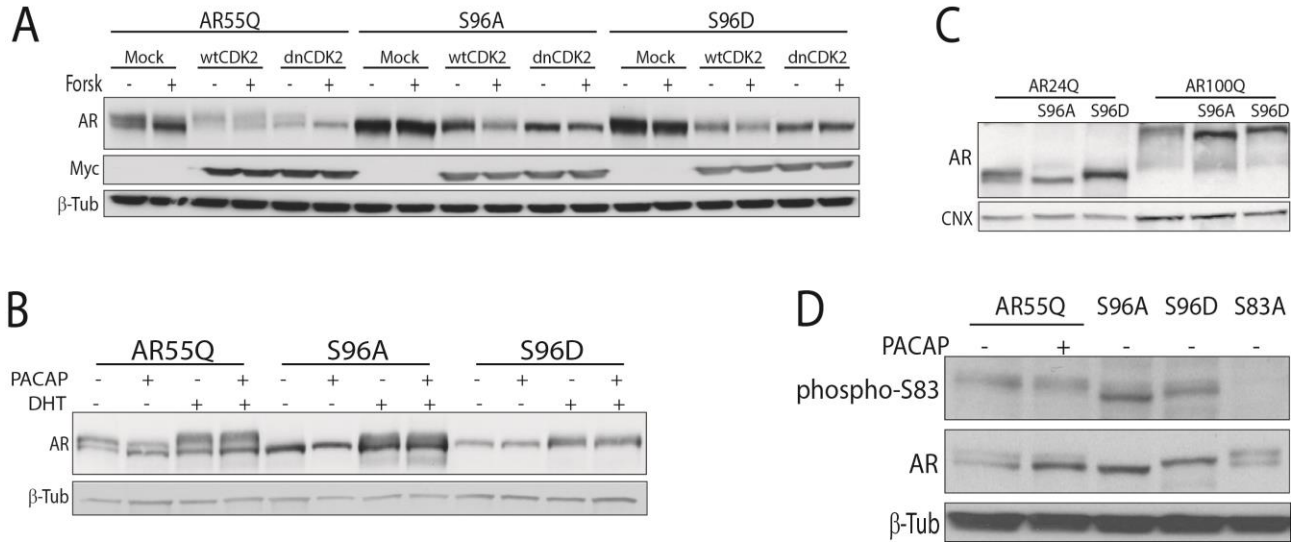


**Fig. S16. Ser$^{96}$ phosphorylation is responsible for the formation of the upper isoform of polyQ-AR.**

A-B) Western blotting analysis in HEK293T cells transfected with vectors expressing AR55Q with and without S96A and S96D substitutions together with empty vector (Mock) and vectors expressing wtCDK2 and dnCDK2. The cells were treated with DHT (10 nM), forskolin (Forsk, 10 μM), and PACAP (100 nM) for 5 h. AR55Q-S96A and AR55Q-S96D run as the lower and upper AR isoforms, respectively. Forskolin, PACAP, and overexpression of wtCDK2 and dnCDK2 did not modify the accumulation of the upper isoform of polyQ-AR with alanine and aspartate substitutions at serine 96.

C) Western blotting analysis in MN-1 cells stably expressing AR24Q and AR100Q with and without S96A and S96D substitutions.

D) Western blotting analysis in HEK293T cells transfected with vectors expressing AR55Q with and without S96A, S96D, and S83A substitutions and treated with PACAP (100 nM) for 5 h. Substitution of serine 96 with alanine and aspartate did not alter phosphorylation at serine 83.

Serine 83-phosphorylated and total AR were detected with specific antibodies, and beta-tubulin (β-Tub) and calnexin (CNX) were used as loading control. *N* = 3 independent experiments.

**Fig. S17**

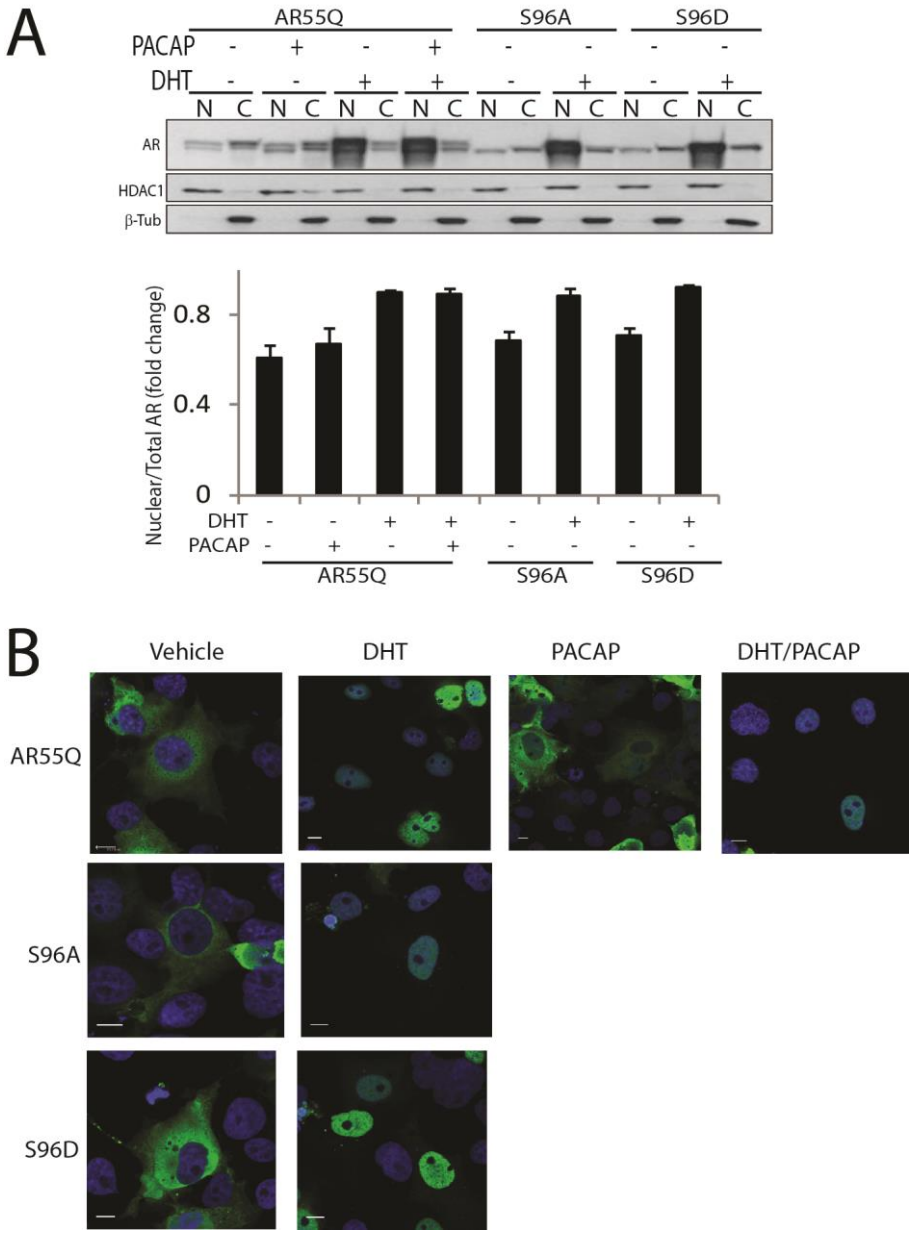


**Fig. S17. Phosphodefective and phosphomimetic substitution of Ser$^{96}$ does not affect polyQ-AR subcellular localization.**

A) Nuclear (N) and cytosolic (C) fractions were collected from HEK293T cells transfected with AR55Q, AR55Q-S96A, and AR55Q-S96D phospho-mutants and treated with vehicle, DHT (10 nM), and PACAP (100 nM) for 5 h. Histone deacetylase 1 (HDAC1) and beta-tubulin (β-Tub) were used as nuclear and cytosolic markers, respectively. Graph, mean ± SEM, $N$ = 4 independent experiments.

B) Representative images of the indicated AR55Q variants in COS7 cells treated with vehicle, DHT (10 nM), and PACAP (100 nM) for 5 h. Treatment of the cells with DHT resulted in nuclear translocation independently of AR phosphorylation at serine 96. AR was detected with a specific antibody, and nuclei were stained with DAPI. *N=?* Scale bar, 10 μm.

**Fig. S18**

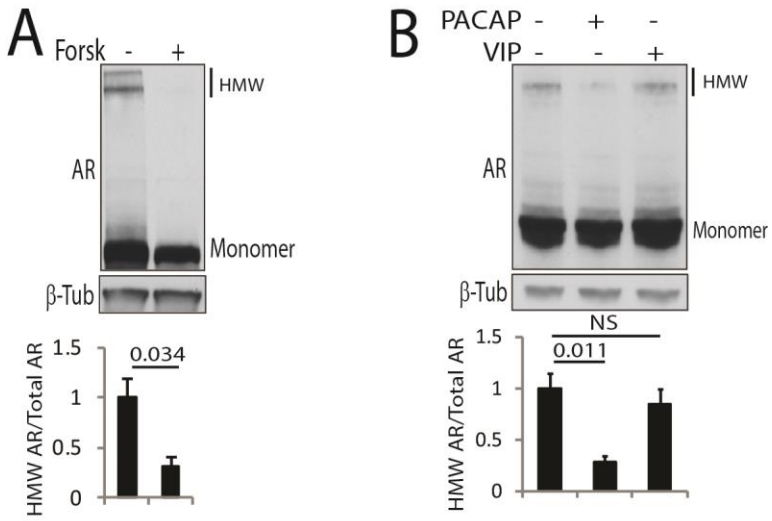


**Fig. S18. Forskolin and PACAP, and not VIP, reduce polyQ-AR aggregation.**
A-B) Western blotting analysis of AR55Q in HEK293T cells treated with forskolin (Forsk, 10 μM), PACAP (100 nM), and VIP (100 nM) for 5 h. Forskolin and PACAP, but not VIP, reduced the accumulation of polyQ-AR into high molecular weight (HMW) species. AR was detected with a specific antibody, and beta-tubulin (β-Tub) was used as loading control. Graph, mean ± SEM, *N* = 3 (A), 2-6 (B) independent experiments. NS, non-significant. Student's t test (A), one-way ANOVA (B).

**Fig. S19**

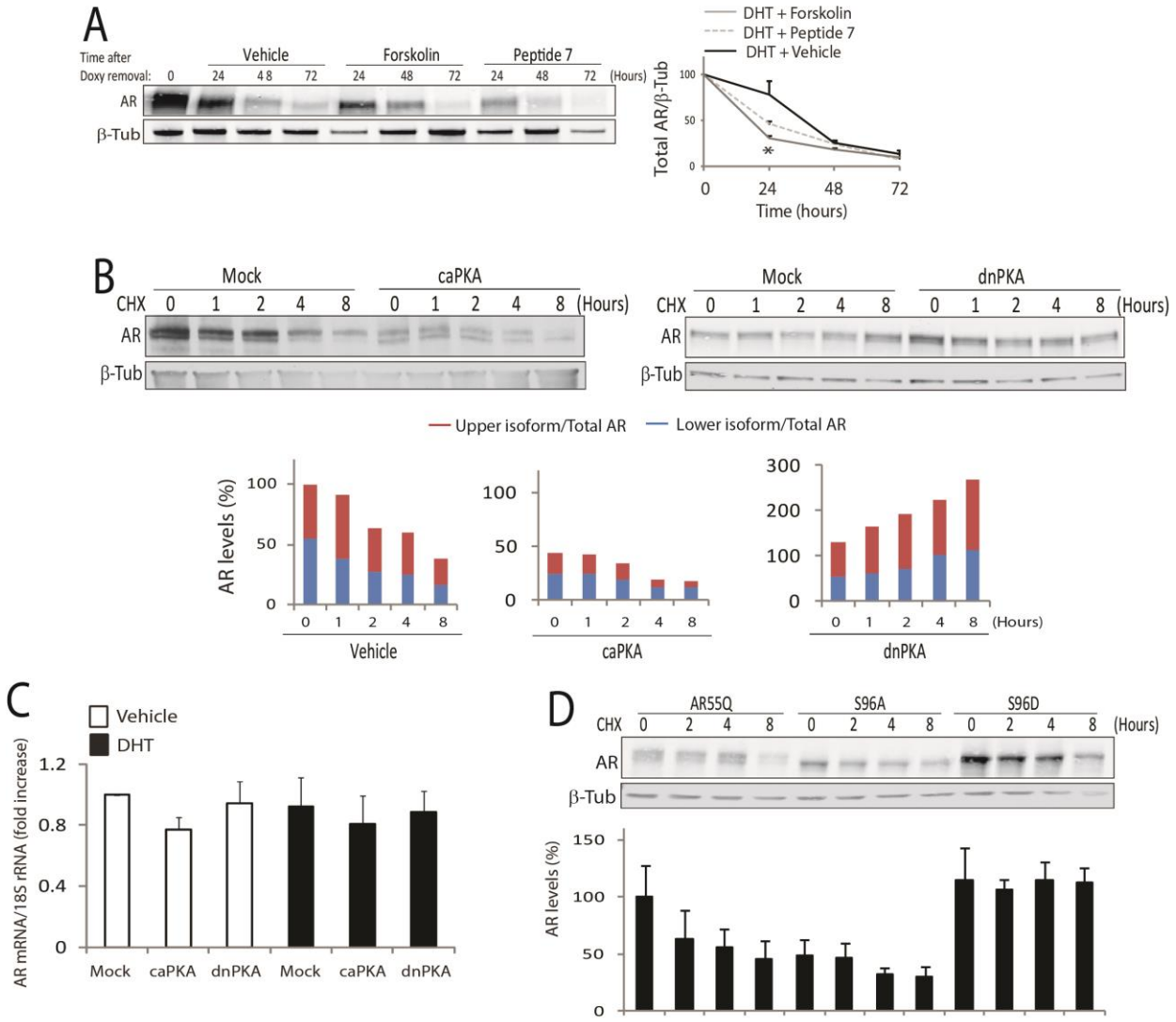


**Fig. S19. Activation of the AC/PKA signaling increases the turnover of polyQ-AR.**

A) Western blotting analysis of AR112Q levels in doxycycline-inducible PC12 cells treated with DHT (10 nM), forskolin (10 μM), and peptide 7 (100 nM) upon removal of doxycycline (Doxy, 10 μg/ml). Forskolin and peptide 7 increased the turnover of polyQ-AR. *N* = 4 independent experiments, * p = 0.001.

B) Western blotting analysis of AR55Q turnover in HEK293T cells transfected with empty vector (mock) or vector expressing either caPKA or dnPKA, and treated with cycloheximide (CHX, 10 μg/ml). caPKA increased the turnover of polyQ-AR, and dnPKA had the opposite effect. *N* = 4 independent experiments.

C) Real-time PCR analysis of the transcript levels of human *AR* in HEK293T cells expressing AR55Q together with either caPKA or dnPKA and normalized to *18S* rRNA. Overexpression of caPKA and dnPKA did not modify the transcript levels of AR55Q. *N* = 3 independent experiments.

D) Western blotting analysis of AR55Q, AR55Q-S96A, and AR55Q-S96D in HEK293T treated as in (B). *N* = 3-4 independent experiments.

AR was detected with a specific antibody, and beta-tubulin (β-Tub) was used as loading control. Graph, mean ± SEM, one-way ANOVA.

**Fig. S20**

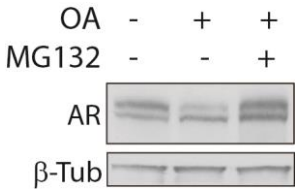


**Fig. S20. OA reduces the accumulation of phosphorylated polyQ-AR by inducing degradation through the UPS.**

Western blotting analysis of AR55Q in HEK293T cells treated with the proteasome inhibitor MG132 (10 μM) and okadaic acid (OA, 100 nM) for 5 h. *N* = 3 independent experiments

**Fig. S21**

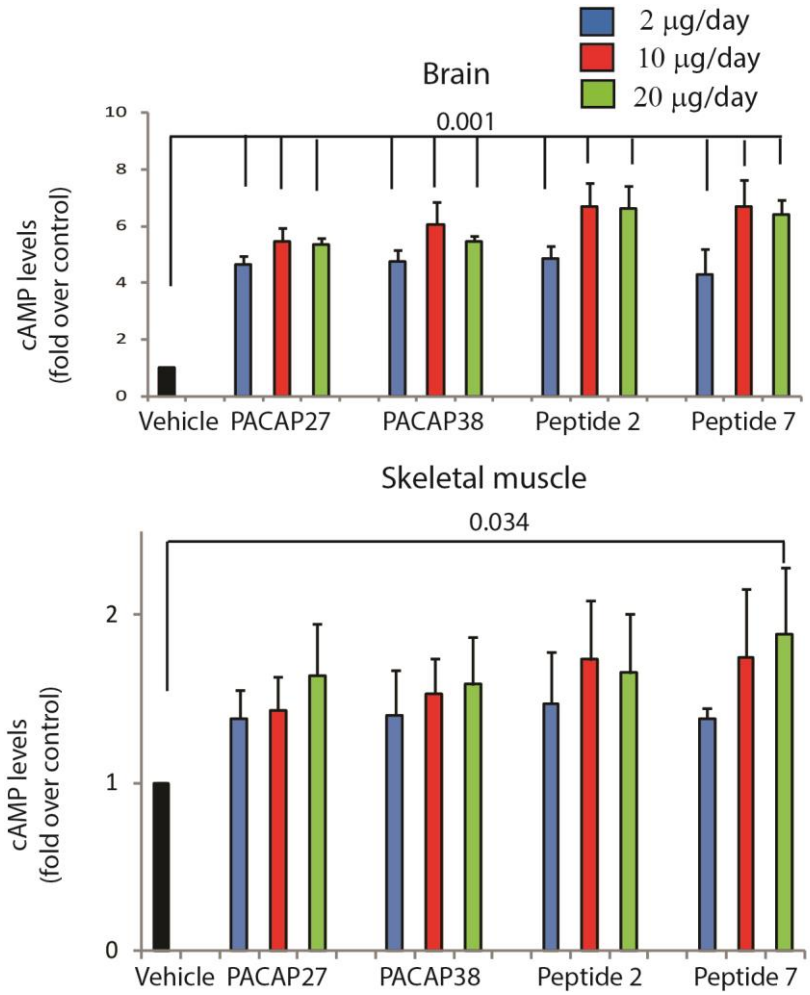


**Fig. S21. PACAP induces cAMP production in vivo.**
cAMP level analysis in tissues of control mice treated with PACAP27, PACAP38, peptide 2, and peptide 7. Intranasal administration of peptide 7 increased cAMP levels in the brain and quadriceps muscle. Graph, mean ± SEM, $N = 3$ mice for each group.

**Fig. S22**

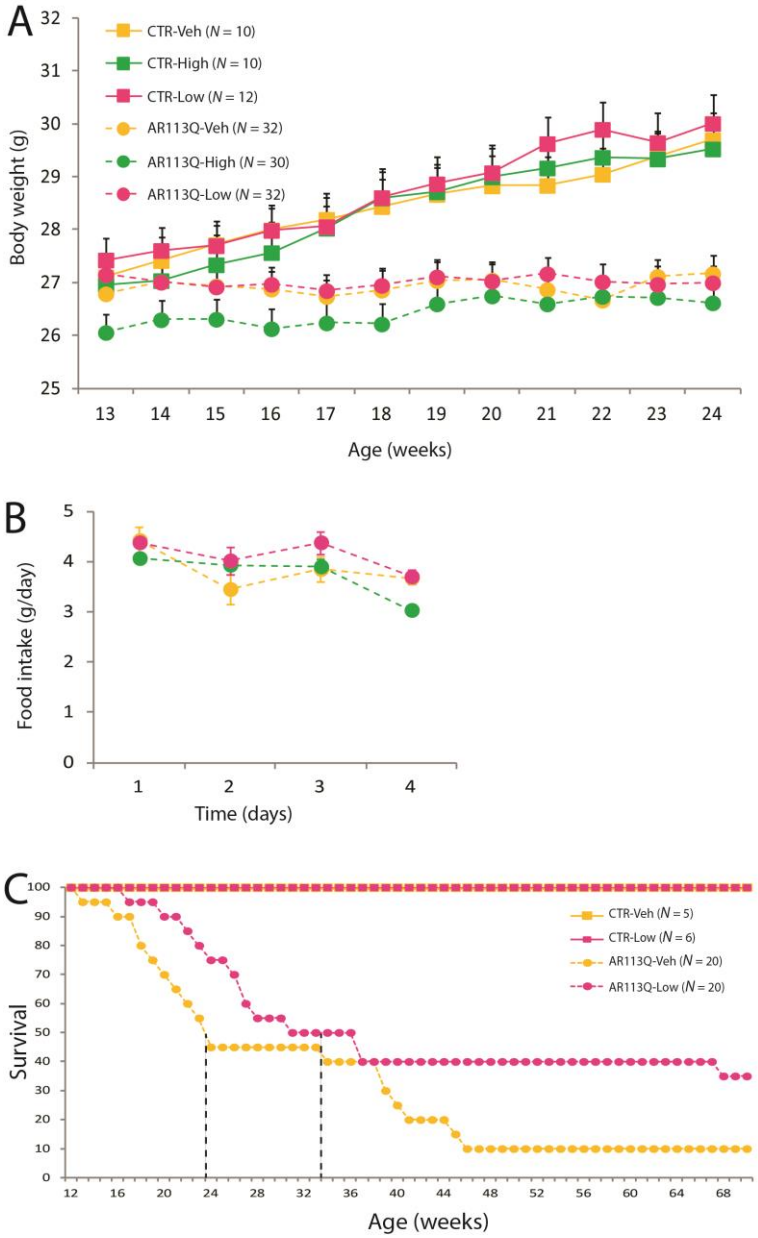


**Fig. S22. Effect of intranasal administration of peptide 7 on body weight, food intake, and survival of AR113Q mice.**

A) Body weight analysis of control (CTR, wild type) and AR113Q mice upon intranasal administration of vehicle (yellow), low (2 μg/day, pink), and high (10 μg/day, green) concentrations of peptide 7. The body weight of AR113Q mice was lower compared to age-matched control littermates and was not modified by peptide 7. Graph, mean ± SEM.

B) Food intake analysis of AR113Q mice treated with vehicle and peptide 7 revealed that treatment of AR113Q mice with peptide 7 does not alter feeding behavior. Graph, mean ± SEM, $N$ = 5 mice for each group.

C) Kaplan-Meier analysis of survival of control and AR113Q mice treated with either vehicle or low dose of peptide 7 revealed that survival of AR113Q mice is ameliorated by treatment of the mice with low dose of peptide 7 ($\chi$2-log rank = 3.293, $P$ =0.069). Even if the effect of low-dose peptide 7 was not significant, it showed a trend for significance.

**Fig. S23**

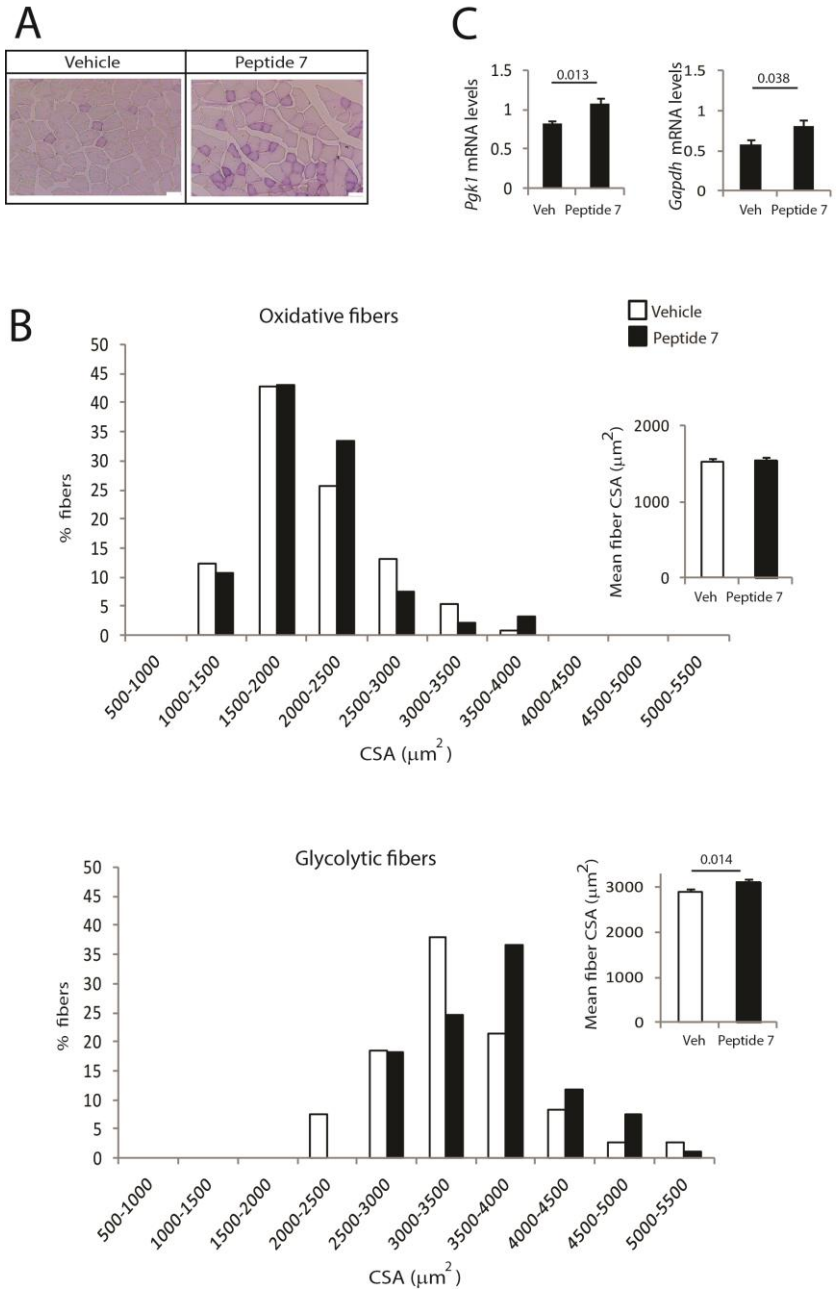


**Fig. S23. Peptide 7 increases the CSA of glycolytic fibers in the skeletal muscle of AR113Q mice and restores the expression of glycolytic genes to normal levels.**

A) NADH representative images from 180-day-old control (CTR, wild type) mice treated as indicated. Bar, 100 μM.

B) NADH staining and analysis of the distribution and mean myofiber CSA of quadriceps oxidative and glycolytic fibers of 180-day-old AR113Q mice treated with either vehicle or peptide 7 (10 μg/day). AR113Q veh *N*=4 mice; AR113Q peptide 7 *N*=3 mice; number of fibers AR113Q veh *N*= 237; AR113Q peptide 7 *N*=195.

C) Real-time PCR analysis of the transcript levels of *Pgk1* and *Gapdh* in the quadriceps of 180-day-old AR113Q mice treated with vehicle (veh) and peptide 7 and normalized to beta-actin. *N* = 3-6 mice for each group.

Graph, mean ± SEM, Student's t test.

**Fig. S24**

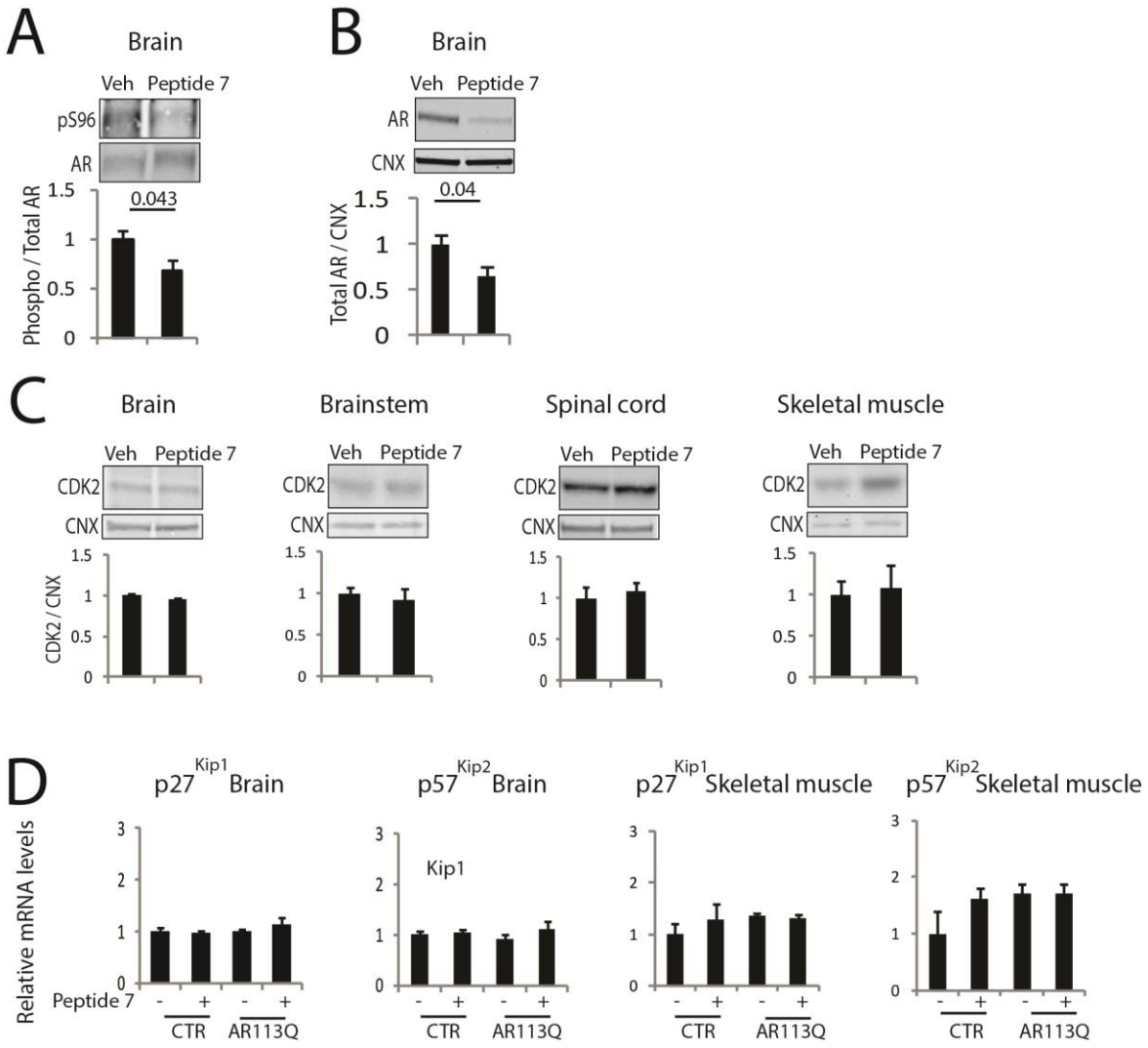


**Fig. S24. Intranasal administration of peptide 7 decreases polyQ-AR phosphorylation and accumulation in SBMA mice without altering CDK2, p27$^{Kip1}$, and p57$^{Kip2}$ expression levels.**

A-C) Western blotting analysis of S96-phosphorylated (A) and total (B) AR, and CDK2 (C) in 180-day-old AR113Q mice treated with either vehicle (veh) or peptide 7 (10 μg/day). AR and CDK2 were detected with specific antibodies, and calnexin (CNX) was used as loading control. Graph, mean ± SEM, *N* = 6 vehicle- and 5 peptide 7-treated mice. Student's t test.

D) Real-time PCR analysis of the transcript levels of the indicated genes in 180-day-old CTR and AR113Q mice treated with vehicle and peptide 7, and normalized to beta-actin. Treatment did not alter the expression of the CDK2 inhibitors, *p27$^{Kip1}$* and *p57$^{Kip2}$*. Graph, mean ± SEM, *N* = 3-6 mice for each group. Two-way ANOVA.

**Fig. S25. Data presented for experiments with sample sizes of less than 20.**

**Figure 1A**

| group | treat | value |
|---|---|---|
| AR24Q | veh | 64.61355 |
| AR24Q | veh | 60.89108 |
| AR24Q | veh | 52.74321 |
| AR24Q | DHT | 75.65177 |
| AR24Q | DHT | 67.7636 |
| AR24Q | DHT | 57.93006 |
| AR65Q | veh | 40.60036 |
| AR65Q | veh | 58.67084 |
| AR65Q | veh | 55.51598 |
| AR65Q | veh | 58.99801 |
| AR65Q | veh | 65.09722 |
| AR65Q | DHT | 56.94792 |
| AR65Q | DHT | 70.62559 |
| AR65Q | DHT | 53.01864 |
| AR65Q | DHT | 73.36956 |
| AR65Q | DHT | 79.82488 |

**Figure 1B**

| group | value |
|---|---|
| AR55Q | 51.45065 |
| AR55Q | 60.15116 |
| AR55Q | 45.94778 |
| AR55QLambda | 4.568691 |
| AR55QLambda | 3.087861 |
| AR55QLambda | 5.287453 |
| AR55QDHT | 69.26399 |
| AR55QDHT | 60.20006 |

| | |
|---|---|
| AR55QDHTLambda | 3.663073 |
| AR55QDHTLambda | 4.231302 |

**Figure 1C**

| group | value |
|---|---|
| AR55Q | 56.77261 |
| AR55Q | 57.31843 |
| AR55Q | 56.50647 |
| AR55QwtPKA | 21.68686 |
| AR55QwtPKA | 17.84117 |
| AR55QwtPKA | 28.9492 |
| AT55QcaPKA | 28.38596 |
| AT55QcaPKA | 32.24674 |
| AT55QcaPKA | 35.51118 |
| AR55qdnPKA | 62.01565 |
| AR55qdnPKA | 63.53845 |
| AR55qdnPKA | 51.39946 |

**Figure 1D**

| group | value |
|---|---|
| veh | 48.05706 |
| veh | 49.46001 |
| veh | 54.80737 |
| forskolin | 15.96867 |
| forskolin | 17.65367 |
| forskolin | 14.62308 |
| DHT | 35.13415 |
| DHT | 35.81406 |
| DHT | 41.0187 |
| forskolinDHT | 19.9651 |
| forskolinDHT | 25.63933 |
| forskolinDHT | 25.33785 |

**Figure 1E**

| gruop | treat | value |
|---|---|---|
| AR24Q | veh | 72.107 |
| AR24Q | veh | 70.18157 |
| AR24Q | veh | 68.03606 |
| AR24Q | forsk | 26.51062 |
| AR24Q | forsk | 35.33785 |
| AR24Q | forsk | 32.95067 |

| | | |
|---|---|---|
| AR100Q | veh | 73.45444 |
| AR100Q | veh | 75.11347 |
| AR100Q | veh | 68.00568 |
| AR100Q | forsk | 57.74464 |
| AR100Q | forsk | 56.9766 |
| AR100Q | forsk | 47.1267 |

**Figure 1F**

| group | treat | value |
|---|---|---|
| AR24Q | veh | 71.45969 |
| AR24Q | veh | 76.43526 |
| AR24Q | veh | 80.78177 |
| AR24Q | veh | 75.56328 |
| AR24Q | forsk | 50.19038 |
| AR24Q | forsk | 40.78764 |
| AR24Q | forsk | 52.03635 |
| AR24Q | forsk | 39.09377 |
| AR100Q | veh | 66.07243 |
| AR100Q | veh | 76.0665 |
| AR100Q | veh | 68.90935 |
| AR100Q | veh | 67.58313 |
| AR100Q | forsk | 48.51305 |
| AR100Q | forsk | 41.35045 |
| AR100Q | forsk | 49.3337 |
| AR100Q | forsk | 44.49002 |

**Figure 2G**

| group | value |
|---|---|
| AR100QDHT | 1 |
| AR100QDHT | 0.4198 |
| AR100QDHT | 0.4349 |
| AR100QDHTforsk | 1.0428 |
| AR100QDHTforsk | 0.5411 |
| AR100QDHTforsk | 0.6949 |
| AR100QDHTpacap | 0.6498 |
| AR100QDHTpacap | 0.4089 |
| AR100QDHTpacap | 0.5821 |

**Figure 3A**

| group | value |
|---|---|
| veh | 62.67598 |

| | |
|---|---|
| veh | 43.63408 |
| veh | 57.54426 |
| inh | 34.32685 |
| inh | 38.99361 |
| inh | 27.53776 |

**Figure 3B**

| group | value |
|---|---|
| mock | 51.95686 |
| mock | 49.47315 |
| mock | 46.91003 |
| mockFork | 24.58667 |
| mockFork | 21.45491 |
| mockFork | 21.79211 |
| wtcdk2 | 63.93148 |
| wtcdk2 | 66.06152 |
| wtcdk2 | 66.58536 |
| wtcdk2Forsk | 59.10957 |
| wtcdk2Forsk | 53.50074 |
| wtcdk2Forsk | 49.49958 |
| dncdk2 | 41.36745 |
| dncdk2 | 36.5945 |
| dncdk2 | 34.24577 |
| dncdk2Forsk | 20.28015 |
| dncdk2Forsk | 6.624609 |
| dncdk2Forsk | 12.72713 |

**Figure 3C**

| group | value |
|---|---|
| mock | 45.29962 |
| mock | 60.61409 |
| mock | 59.69844 |
| mockpacap | 12.90056 |
| mockpacap | 42.88333 |
| mockpacap | 46.02248 |
| cdk2 | 71.00053 |
| cdk2 | 60.08351 |
| cdk2 | 66.37873 |
| cdk2pacap | 60.96065 |
| cdk2pacap | 57.708 |
| cdk2pacap | 61.7661 |

**Figure 3E**

| GROUP | VALUE |
|---|---|
| Mock-A | 0.462458 |
| Mock-A | 17.18238 |
| AR55Q-A | 2.591437 |
| AR55Q-A | 13.16989 |
| S96A-A | 1.009827 |
| S96A-A | 9.731839 |
| 8A-A | 1.139224 |
| 8A-A | 11.95511 |
| Mock-E | 1.714967 |
| Mock-E | 13.48413 |
| AR55Q-E | 100 |
| AR55Q-E | 100 |
| S96A-E | 14.19443 |
| S96A-E | 18.85929 |
| 8A-E | 176.9992 |

**Figure 3H**

| group | value |
|---|---|
| veh | 1.033299 |
| veh | 1.023615 |
| veh | 0.943086 |
| OA | 0.524224 |
| OA | 0.723362 |
| OA | 0.376426 |

**Figure 3I**

| group | value |
|---|---|
| veh | 56.01289 |
| veh | 56.31387 |
| veh | 59.65272 |
| OA | 38.71984 |
| OA | 42.09039 |
| OA | 48.8959 |
| siRNA | 61.11262 |
| siRNA | 70.61352 |
| siRNA | 63.51175 |
| OAsiRNA | 67.63696 |
| OAsiRNA | 69.2243 |
| OAsiRNA | 64.87957 |

**Figure 3J**

| group | value |
|---|---|
| veh | 51.24308 |
| veh | 54.93386 |
| veh | 50.71006 |
| forsk | 35.61421 |
| forsk | 40.05759 |
| forsk | 41.76834 |
| pacap | 40.5925 |
| pacap | 40.91067 |
| pacap | 44.12021 |
| vehsi | 51.60008 |
| vehsi | 52.09947 |
| vehsi | 51.70886 |
| forsk-si | 53.78707 |
| forsk-si | 54.65492 |
| forsk-si | 55.28472 |
| pacap-si | 53.75065 |
| pacap-si | 51.33402 |
| pacap-si | 54.90776 |

**Figure 4D**

| GROUP | VALUE |
|---|---|
| VEH | 0.930105 |
| VEH | 1.2271 |
| VEH | 0.634977 |
| VEH | 1.545337 |
| VEH | 0.66248 |
| FORSK | 0.370212 |
| FORSK | 0.263451 |
| FORSK | 0.157497 |
| FORSK | 0.363956 |
| FORSK | 0.517303 |

**Figure 4G**

| GROUP | VALUE |
|---|---|
| AR100Q | 0.675935 |
| AR100Q | 1.36768 |
| AR100Q | 0.956385 |
| AR100Q-S96A | 0.380767 |
| AR100Q-S96A | 0.393239 |

| | |
|---|---|
| AR100Q-S96A | 0.472027 |

**Figure 5A**

| group | value |
|---|---|
| DHT | 1.058325 |
| DHT | 0.884066 |
| DHT | 1.057609 |
| DHTforsk | 0.618815 |
| DHTforsk | 0.558673 |
| DHTforsk | 0.744951 |

**Figure 6B**

| group | value |
|---|---|
| vehicle | 1.080807 |
| vehicle | 1.050271 |
| vehicle | 0.868922 |
| 2peptide | 1.455574 |
| 2peptide | 1.287667 |
| 2peptide | 1.202684 |
| 4peptide | 1.424531 |
| 4peptide | 1.295365 |
| 4peptide | 1.201615 |
| 7peptide | 1.418114 |
| 7peptide | 1.23204 |
| 7peptide | 1.253271 |
| PACAP | 1.183957 |
| PACAP | 1.161921 |
| PACAP | 1.131423 |

**Figure 7D-Musk**

| group | treat | value |
|---|---|---|
| wt | veh | 0.97199053433859 |
| wt | veh | 0.93285437882211 |
| wt | veh | 1.10286945816958 |
| wt | P7 | 1.90083757978007 |
| wt | P7 | 1.81913414356073 |
| wt | P7 | 1.10209104028611 |
| 113Q | veh | 2.82029337080158 |
| 113Q | veh | 1.63689492991979 |
| 113Q | veh | 2.40876746799678 |
| 113Q | veh | 1.46538115532798 |
| 113Q | veh | 2.22023583439639 |
| 113Q | veh | 2.18670611471188 |
| 113Q | P7 | 3.83220573511134 |
| 113Q | P7 | 3.58351843746970 |

| | | |
|---|---|---|
| 113Q | P7 | 2.82612132499574 |
| 113Q | P7 | 4.02240786353928 |
| 113Q | P7 | 3.05997571911348 |

**Figure 7D-Runx**

| geno | treat | value |
|---|---|---|
| wt | veh | 0.758306 |
| wt | veh | 1.281174 |
| wt | veh | 1.029313 |
| wt | P7 | 1.245759 |
| wt | P7 | 1.345625 |
| wt | P7 | 0.780591 |
| 113Q | veh | 2.927901 |
| 113Q | veh | 3.083974 |
| 113Q | veh | 2.193738 |
| 113Q | veh | 2.82466 |
| 113Q | veh | 3.170296 |
| 113Q | veh | 2.360577 |
| 113Q | veh | 3.843749 |
| 113Q | veh | 2.950441 |
| 113Q | veh | 4.55314 |
| 113Q | P7 | 1.627178 |
| 113Q | P7 | 2.466153 |
| 113Q | P7 | 2.513704 |
| 113Q | P7 | 2.347338 |
| 113Q | P7 | 2.453679 |
| 113Q | P7 | 2.776789 |
| 113Q | P7 | 3.397519 |
| 113Q | P7 | 2.562199 |
| 113Q | P7 | 2.146592 |

**Figure 7D-NR4A1**

| geno | treat | value |
|---|---|---|
| ctr | veh | 0.829882 |
| ctr | veh | 1.082256 |
| ctr | veh | 1.113406 |
| ctr | P7 | 1.188319 |
| ctr | P7 | 1.294393 |
| ctr | P7 | 0.704257 |
| AR113Q | veh | 0.442839 |
| AR113Q | veh | 0.565471 |
| AR113Q | veh | 0.279268 |
| AR113Q | veh | 0.43694 |
| AR113Q | veh | 0.429924 |
| AR113Q | veh | 0.432277 |
| AR113Q | P7 | 0.916113 |
| AR113Q | P7 | 1.0486 |
| AR113Q | P7 | 0.844213 |
| AR113Q | P7 | 0.34434 |
| AR113Q | P7 | 0.435094 |

**Figure 8A-Brainstem**

| TREAT | VALUE |
|---|---|
| VEH | 1.00813 |
| VEH | 0.968293 |

| | |
|---|---|
| VEH | 1.171252 |
| VEH | 1.038694 |
| VEH | 0.997491 |
| VEH | 0.816139 |
| P7 | 0.775883 |
| P7 | 0.764594 |
| P7 | 0.672096 |
| P7 | 0.73033 |
| P7 | 0.755427 |

**Figure 8A-Spinal cord**

| group | value |
|---|---|
| veh | 0.935092 |
| veh | 0.974224 |
| veh | 1.045049 |
| veh | 1.045635 |
| P7 | 0.812464 |
| P7 | 0.71794 |
| P7 | 0.586372 |
| P7 | 0.925581 |

**Figure 8A-Quadriceps**

| group | value |
|---|---|
| VEH | 0.984916 |
| VEH | 0.894556 |
| VEH | 1.048393 |
| VEH | 1.12763 |
| VEH | 0.880311 |
| VEH | 1.064194 |
| P7 | 0.951503 |
| P7 | 0.617908 |
| P7 | 0.770826 |
| P7 | 0.876331 |
| P7 | 0.756268 |

**Figure 8B-Brainstem**

| group | value |
|---|---|
| veh | 1.038918 |
| veh | 0.911 |
| veh | 0.801594 |
| veh | 0.982986 |

| | |
|---|---|
| veh | 1.202745 |
| veh | 1.062914 |
| P7 | 0.695233 |
| P7 | 0.752206 |
| P7 | 0.61346 |

**Figure 8B- Spinal cord**

| group | value |
|---|---|
| veh | 0.924574 |
| veh | 0.727626 |
| veh | 0.790763 |
| veh | 1.103925 |
| veh | 1.355227 |
| veh | 1.097885 |
| P7 | 0.847616 |
| P7 | 0.490114 |
| P7 | 0.742131 |
| P7 | 0.864832 |
| P7 | 0.609966 |

**Figure 8B-Quadriceps**

| group | value |
|---|---|
| veh | 1.000537 |
| veh | 1.032252 |
| veh | 0.845576 |
| veh | 0.780098 |
| veh | 1.165167 |
| veh | 1.17637 |
| P7 | 0.986917 |
| P7 | 0.649521 |
| P7 | 0.676404 |
| P7 | 0.622728 |
| P7 | 0.581452 |

**Figure 8C-Brainsteim**

| group | value |
|---|---|
| veh | 1.12054063681540 |
| veh | 0.55504621017770 |
| veh | 1.11177355691888 |
| veh | 1.44711360598648 |
| veh | 1.38594945932822 |
| veh | 0.93020225482736 |
| P7 | 1.97985612296188 |
| P7 | 1.49633932074617 |

| | |
|---|---|
| P7 | 1.23300842801230 |
| P7 | 1.59367555720856 |
| P7 | 1.47751582242848 |

**Figure 8C-Spinal cord**

| group | value |
|---|---|
| veh | 1.073 |
| veh | 0.936 |
| veh | 0.872 |
| veh | 1.217 |
| veh | 1.047 |
| veh | 0.699 |
| P7 | 1.231 |
| P7 | 1.308 |
| P7 | 1.170 |
| P7 | 1.340 |

**Figure 8C-Quadriceps**

| group | value |
|---|---|
| veh | 1.995314 |
| veh | 1.449585 |
| veh | 1.087341 |
| veh | 1.317243 |
| veh | 2.15196 |
| veh | 1.280981 |
| P7 | 2.065152 |
| P7 | 2.471766 |
| P7 | 2.84046 |
| P7 | 2.659396 |
| P7 | 2.076294 |

**Figure S1**

| group | value |
|---|---|
| AR55Q | 52.38728 |
| AR55Q | 69.10875 |
| AR55Q | 54.57804 |
| AR55Qlambda | 4.032082 |
| AR55Qlambda | 4.585267 |
| AR55Qlambda | 9.283778 |
| AR55QcaPKA | 18.86977 |
| AR55QcaPKA | 27.16672 |
| AR55QcaPKA | 15.02803 |
| AR55QcaPKAlambda | -1.81743 |
| AR55QcaPKAlambda | 3.664756 |
| AR55QcaPKAlambda | 11.0601 |

**Figure S6C**

| group | value |
|---|---|

| | |
|---|---|
| AR55Q | 51.16187 |
| AR55Q | 57.30437 |
| AR55Q | 45.70833 |
| AR55Qforsk | 21.27907 |
| AR55Qforsk | 19.90788 |
| AR55Qforsk | 14.40095 |
| cdk1 | 52.84058 |
| cdk1 | 60.44314 |
| cdk1 | 41.58285 |
| cdk1Forsk | 30.45949 |
| cdk1Forsk | 27.27467 |
| cdk1Forsk | 26.89848 |
| dncdk1 | 45.98368 |
| dncdk1 | 53.4518 |
| dncdk1 | 48.94224 |
| dncdk1Forsk | 14.16013 |
| dncdk1Forsk | 12.68314 |
| dncdk1Forsk | 11.6148 |

**Figure S6D**

| geno | TREATMENT | VALUE |
|---|---|---|
| AR55Q VEH | VEH | 1.041001 |
| AR55Q VEH | VEH | 0.97228 |
| AR55Q VEH | VEH | 0.986719 |
| AR55Q FORS | FORS | 0.908217 |
| AR55Q FORS | FORS | 0.835231 |
| AR55Q FORS | FORS | 0.853947 |
| AR55Q CDK5  VEH | VEH | 1.14193 |
| AR55Q CDK5  VEH | VEH | 1.014026 |
| AR55Q CDK5  VEH | VEH | 1.076979 |
| AR55Q CDK5  FORS | FORS | 0.911366 |
| AR55Q CDK5  FORS | FORS | 0.667618 |
| AR55Q CDK5  FORS | FORS | 0.824989 |
| AR55Q CDK5 DN VEH | VEH | 0.923656 |
| AR55Q CDK5 DN VEH | VEH | 0.85451 |
| AR55Q CDK5 DN VEH | VEH | 0.939583 |
| AR55Q CDK5 DN FORS | FORS | 0.829978 |
| AR55Q CDK5 DN FORS | FORS | 0.647844 |
| AR55Q CDK5 DN FORS | FORS | 0.735882 |

**Figure S6E- CDK1**

| group | value |
|---|---|
| sc | 1.049442 |

| | |
|---|---|
| sc | 0.950558 |
| 2sh | 0.820284 |
| 2sh | 0.545235 |
| 3sh | 0.571403 |
| 3sh | 0.578556 |

**Figure S6E-AR**

| group | value |
|---|---|
| sc | 57.68844 |
| sc | 57.96591 |
| 2sh | 61.93548 |
| 2sh | 59.69266 |
| 3sh | 58.32193 |
| 3sh | 49.33665 |

**Figure S13A**

| geno | treat | value |
|---|---|---|
| AR12Q | veh | 100 |
| AR12Q | veh | 100 |
| AR12Q | veh | 100 |
| AR12Q | veh | 100 |
| AR12Q | OA | 136.5645 |
| AR12Q | OA | 127.6972 |
| AR12Q | OA | 125.4959 |
| AR12Q | OA | 129.2315 |

| geno | treat | value |
|---|---|---|
| AR55Q | veh | 100 |
| AR55Q | veh | 100 |
| AR55Q | veh | 100 |
| AR55Q | veh | 100 |
| AR55Q | OA | 110.7856 |
| AR55Q | OA | 114.5084 |
| AR55Q | OA | 112.3098 |
| AR55Q | OA | 140.2581 |

**Figure S18A**

| group | value |
|---|---|
| veh | 1.382302 |
| veh | 0.754637 |
| veh | 0.863061 |
| forsk | 0.263685 |

| | |
|---|---|
| forsk | 0.180313 |
| forsk | 0.506954 |

**Figure S18B**

| group | value |
|---|---|
| veh | 0.387492 |
| veh | 0.898281 |
| veh | 1.213883 |
| veh | 1.457384 |
| veh | 1.044506 |
| veh | 0.998453 |
| pacap | 0.024613 |
| pacap | 0.013652 |
| pacap | 0.319331 |
| pacap | 1.112963 |
| pacap | 0.391464 |
| pacap | 0.229858 |
| vip | 1.041156 |
| vip | 0.687807 |

**Figure S24A**

| group | value |
|---|---|
| VEH | 0.69684 |
| VEH | 0.946757 |
| VEH | 1.247372 |
| VEH | 1.136663 |
| VEH | 0.848022 |
| VEH | 1.124347 |
| P7 | 0.458967 |
| P7 | 0.637935 |
| P7 | 1.073778 |
| P7 | 0.507454 |
| P7 | 0.73606 |

**Figure S24B**

| group | value |
|---|---|
| VEH | 1.084487 |
| VEH | 1.214291 |
| VEH | 0.66745 |
| VEH | 0.769172 |
| VEH | 0.960789 |

| | |
|---|---|
| VEH | 1.303811 |
| P7 | 0.810724 |
| P7 | 0.990796 |
| P7 | 0.466989 |
| P7 | 0.414671 |
| P7 | 0.545162 |

**Figure S24C-Brain**

| group | value |
|---|---|
| veh | 1.082829 |
| veh | 0.986177 |
| veh | 0.97859 |
| veh | 0.905549 |
| veh | 0.906052 |
| veh | 1.140804 |
| p7 | 0.978738 |
| p7 | 0.953045 |
| p7 | 0.880701 |
| p7 | 0.875824 |
| p7 | 1.050497 |

**Figure S24C-Brainstem**

| group | value |
|---|---|
| VEH | 1.258977 |
| VEH | 0.898151 |
| VEH | 1.104892 |
| VEH | 0.94838 |
| VEH | 0.703191 |
| VEH | 1.08641 |
| P6 | 0.521984 |
| P7 | 1.180288 |
| P7 | 1.080025 |
| P7 | 0.892805 |

**Figure S24C-Spinal cord**

| group | value |
|---|---|
| VEH | 0.807015 |
| VEH | 0.855166 |
| VEH | 0.917293 |
| VEH | 1.420525 |
| P7 | 0.801848 |

| | |
|---|---|
| P7 | 1.213797 |
| P7 | 1.07229 |
| P7 | 1.276142 |

**Figure S24C-Quadriceps**

| group | value |
|---|---|
| VEH | 1.0301 |
| VEH | 1.021649 |
| VEH | 0.459922 |
| VEH | 0.829487 |
| VEH | 1.739783 |
| VEH | 0.919059 |
| P6 | 1.896515 |
| P7 | 1.015766 |
| P7 | 1.218774 |
| P7 | 0.963457 |
| P7 | 0.35197 |